JOURNAL OF VIROLOGY, July 2007, p. 7786–7800 Vol. 81, No. 14
0022-538X/07/$08.00+0 doi:10.1128/JVI.02780-06

Small Interfering RNA Profiling Reveals Key Role of Clathrin-Mediated Endocytosis and Early Endosome Formation for Infection by Respiratory Syncytial Virus▽

Andrey A. Kolokoltsov,[1]† Drew Deniger,[1]† Elisa H. Fleming,[1] Norbert J. Roberts, Jr.,[1] Jon M. Karpilow,[2] and Robert A. Davey[1]*

Department of Microbiology and Immunology, Division of Infectious Diseases, University of Texas Medical Branch, Galveston, Texas,[1] and Dharmacon, Inc., Lafayette, Ohio[2]

Received 15 December 2006/Accepted 1 May 2007

Respiratory syncytial virus (RSV) is a common cause of respiratory tract infections in infants and the elderly. Like many other pH-independent enveloped viruses, RSV is thought to enter at the cell surface, independently of common endocytic pathways. We have used a targeted small interfering RNA (siRNA) library to identify key cellular genes involved in cytoskeletal dynamics and endosome trafficking that are important for RSV infection. Surprisingly, RSV infection was potently inhibited by siRNAs targeting genes associated with clathrin-mediated endocytosis, including clathrin light chain. The important role of clathrin-mediated endocytosis was confirmed by the expression of well-characterized dominant-negative mutants of genes in this pathway and by using the clathrin endocytosis inhibitor chlorpromazine. We conclude that, while RSV may be competent to enter at the cell surface, clathrin function and endocytosis are a necessary and important part of a productive RSV infection, even though infection is strictly independent of pH. These findings raise the possibility that other pH-independent viruses may share a similar dependence on endocytosis for infection and provide a new potential avenue for treatment of infection.

Respiratory syncytial virus (RSV) is a leading cause of respiratory tract infection for people of all ages, but disease is usually limited to the very young and old. Infection may also induce a persistent asthma-like illness (41). Afflicted patients exhibit damage to the upper respiratory tract, the origin of which is believed to be coupled to the host immune response (61). Despite the seriousness of RSV infection, there currently is no vaccine available and only a single drug, the entry inhibitor BMS-433771, has demonstrated therapeutic promise (11). For these reasons, a better understanding of the infection cycle and mechanisms of infection by RSV is necessary to aid the development of improved therapeutic strategies.

RSV is a paramyxovirus with a 15-kb, negative sense, single-stranded RNA genome. Viral particles are present in two forms, a long filamentous variant of up to 1 μm in length and a smaller, spherical particle of 100 nm in diameter. It is unclear which type of particle is most responsible for human respiratory infection. The RSV genome is organized similarly to other paramyxoviruses. Three envelope proteins (G, F, and SH) play a central role in cell entry (32, 55) but, unlike other paramyxoviruses, the F protein of RSV is sufficient for cell attachment and entry. Thus, while the G and SH genes are dispensable in cell culture, they likely play important roles for infection in vivo (29, 53, 54).

Much of our knowledge of the early steps in RSV entry is by analogy to similar enveloped viruses. In general, enveloped viruses are divided into two classes, those for which fusion and entry are triggered by acidic pH and a second group that fuses to the cell membrane at neutral pH. This classification is based primarily on the sensitivity of virus infection to drugs that neutralize endosomal acidification, as well as the sensitivity of infectivity to acidic pH. For many types of virus, including the well-studied vesicular stomatitis virus (VSV) and influenza A virus, a drop in pH is necessary and sufficient to mediate envelope protein structural rearrangements (8, 9, 19, 60) that bring about membrane fusion and delivery of the virus capsid into the cell cytosol (24). For other viruses, like Ebola, the activation of pH-dependent proteases is required to cleave the envelope proteins before structural rearrangement and membrane fusion can occur (10). For such viruses, endocytosis is required to bring the virus into the acidic environment of the early-to-late-stage endosome. The best-studied endocytic pathway involves clathrin-coated pit formation and is controlled by clathrin and the AP2 complex (45). Caveolae form a second class of endocytic vesicle but are less-well characterized and are distinguished by the presence of caveolin instead of clathrin (36). Still a third set of endocytic pathways are neither caveolin nor clathrin associated but may involve Arf-related proteins (37) and, like caveolae, are involved in the uptake of lipid rafts. Each of these endocytic pathways appears to converge on acidified endosomes (38), and drugs that block endosomal acidification can be potent antivirals (56).

In contrast, most retroviruses and paramyxoviruses enter cells irrespective of treatment with drugs that inhibit endosomal acidification. For RSV, membrane fusion and infection of HEp-2 cells were resistant to treatment with a weak base, ammonium chloride, that buffers against acidification (28, 48). This has been interpreted to mean that RSV does not require

* Corresponding author. Mailing address: Department of Microbiology and Immunology, University of Texas Medical Branch, 301 University Blvd., Galveston, TX. Phone: (409) 772-4915. Fax: (409) 772-5065. E-mail: radavey@utmb.edu.
† These authors contributed equally to this work.
▽ Published ahead of print on 9 May 2007.

endocytosis and instead, like other pH-independent viruses, fuses directly with the plasma membrane. In other work, using video microscopy of HEp-2 cells, RSV viral filaments were seen being taken up through the plasma membrane by an undefined macropinocytic mechanism (46). Such uptake would likely require extensive actin and cytoskeleton rearrangement to engulf the viral filament. Unfortunately, this work did not indicate if this adsorption of filaments led to productive infection or, instead, to a dead-end pathway. No similar studies have been reported with spherical particles. It therefore remains unclear what route is used by RSV to productively infect cells.

In the current studies, a novel array of small interfering RNAs (siRNAs) that specifically target genes important for actin polymerization, cytoskeleton rearrangement, and endocytosis were used to determine the entry pathway used by RSV. Surprisingly, we show that the knockdown of genes associated with clathrin-mediated endocytosis efficiently blocks RSV infection. The requirement for endocytosis was confirmed by the expression of dominant-negative mutants that inhibit this uptake pathway. Chlorpromazine, a drug that inhibits clathrin-mediated endocytosis (57), was also an effective inhibitor of RSV infection. Based on these data, we propose a mechanism by which RSV takes advantage of clathrin-mediated endocytosis to gain access to the cytoplasm and we propose that cell surface entry points lead to nonproductive infection.

MATERIALS AND METHODS

Chemicals. All chemicals were ultragrade from Sigma (St. Louis, MO) unless stated otherwise. Dharmafect cell culture reagent and DharmaFECT 1 transfection reagent were from Dharmacon (Lafayette, CO).

Antibodies. Polyclonal serum raised against VSV Indiana strain, obtained from ATCC (VR-1238AF), was used for fluorescence-activated cell sorter (FACS) detection of virus infection. A monoclonal antibody against RSV F protein (MCA490) was obtained from Serotec (Raleigh, NC) and used for the detection of RSV infection by FACS analysis. The secondary antibody was Alexa $Fluor_{647}$-labeled goat anti-mouse immunoglobulin G (A21235) from Invitrogen (Carlsbad, CA). Antibodies for confirmation of siRNA knockdown of protein expression were from Santa Cruz Biotech (Santa Cruz, CA) and were made against unique peptides in the targeted protein. Those that were used in this report were against AP2-alpha (sc-17771), Rab5 (isoforms A, B, and C were sc-309, sc-598, and sc-26570, respectively), clathrin light chain A (sc-28276), clathrin light chain B (sc-28277), dynamin I (sc-12724), dynamin II (sc-6400), PAK-1 (sc-882), or WASF2 (sc-10394). Both anti-dynamin 3 antibody (ab3458) and anti-beta-actin antibody (600-532A1; served as loading control) were from Novus Biologicals, Littleton, CO. Each was detected on blots by using appropriate secondary horseradish peroxidase-conjugated antibodies. Goat anti-mouse (Pierce, Rockford, IL), mouse anti-goat (Pierce), or donkey anti-rabbit (Amersham) antibodies were used where appropriate. Chemiluminescent substrate detection was used to visualize bound antibody on blots (ECL kit; Amersham).

Cell lines and culture conditions. Cells were maintained in a humidified air–5% CO_2 atmosphere incubator at 37°C. 293 FT cells were from Invitrogen. Both 293 and HeLa cells (ATCC CCL-2) were grown in Dulbecco's modified Eagle's medium (Gibco) supplemented with 10% fetal bovine serum (Gemini Bioproducts, West Sacramento, CA).

Virus stocks. VSV Indiana strain was obtained from ATCC (VR-1238). VSV Indiana strain expressing green fluorescent protein (GFP) or dsRed was kindly provided by M. Whitt (University of Alabama). RSV expressing dsRed was provided by M. Peeples and P. Collins (22). Wild-type RSV was from ATCC (VR-26). For RSV cultivation, HeLa cells were grown to 20% confluence and then infected at a multiplicity of infection (MOI) of 0.5. The cells were incubated at 37°C in a CO_2 incubator until a cytopathic effect was observed (typically 2 days postinfection). The culture supernatant was harvested and cell debris was pelleted for 5 min at 3,000 × *g*. The supernatant was used immediately or stored frozen at −80°C. For VSV, 293 cells were grown to 80% confluence and infected at an MOI of 0.5. The culture supernatant was collected the following day and filtered through a 0.45-μm syringe filter to remove cell debris. Virus was used immediately or stored frozen at −80°C.

GFP, red fluorescent protein, or virus envelope protein expression was used to monitor infection by each virus. For VSV, infection was detected 7 h after infection. For RSV, marker expression was detected 20 h postinfection. Infected cells were counted by using a Leica DMIRB inverted epifluorescence microscope.

Production of envelope protein-pseudotyped murine leukemia virus. Virus envelope protein-pseudotyped murine leukemia viruses (MLV) were prepared as controls in the drug treatment experiments and for FACS analysis of virus infection. Pseudotypes were made bearing the envelope proteins of VSV type G (VSV-G), ecotropic MLV, or 10A1 MLV. Both the VSV-G- and ecotropic MLV-pseudotyped viruses encoded GFP as a marker of infection. The 10A1-pseudoyped virus encoded either GFP or a truncated CD4 (CD4.1) marker (Miltenyi Biotec, Auburn, CA) of infection. The latter was cloned into the retroviral packaging plasmid pFB (Stratagene, La Jolla, CA). Pseudotyped virus was assembled by transfecting 293 FT cells (Invitrogen) with plasmids encoding the MLV core structural proteins (pGag-Pol) together with plasmids carrying the reporter gene (pΨ-GFP or pFB-CD4.1) and encoding the envelope protein of VSV (pVSV-G; Clontech, Mountain View, CA); ecotropic MLV (pcDNA3:Fr-env), as detailed elsewhere (30); or p10A1 (Clontech, Mountain View, CA). Calcium phosphate was used as the method of plasmid transfection. After 2 days, culture supernatants were collected and filtered through a 0.45-μm filter to remove cell debris, and the filtered virus was used immediately or stored frozen at −80°C. The expression of GFP was detected 36 h postinfection by counting fluorescent cells by microscopy.

Drug treatments. To confirm the pH independence of RSV infection, cells were treated with lysosomotropic agents which inhibit endosomal acidification. VSV (a pH-dependent virus) and ecotropic MLV (a pH-independent virus) were used as controls. Cells were incubated for 1 h in the presence of chloroquine (10 μM), ammonium chloride (10 mM), or bafilomycin A1 (10 nM). Virus was then added, and each compound was maintained with cells for a further 5 h. If a drug inhibited virus infection, it was expected that this time of incubation would limit cell toxicity but delay infection sufficiently to reduce the virus titer to undetectable levels. The culture medium was then removed, and cells were cultivated for the times indicated below. In each case, the viruses, including RSV, encoded GFP as a marker of infection and the virus titer was determined by counting the GFP-positive cells after virus challenge.

Chlorpromazine was used to block clathrin-mediated endocytosis. Cells were treated as described above, with the indicated concentrations of the drug. Again, a VSV-G-pseudotyped virus was used as a clathrin-dependent control. 10A1 MLV was previously reported to be unaffected by chlorpromazine, and so, a pseudotype of this virus expressing GFP as a marker of infection was used to control for drug toxicity.

siRNA library. The siRNA library used was a subset of the membrane-trafficking siRNA library (RTF H-005500; Dharmacon). Pools of four siRNAs targeting each gene were initially tested. A pooled approach allowed the identification of potentially important genes without requiring the testing of each siRNA individually. The other advantage is that combined siRNAs may work synergistically by targeting distinct regions of the same mRNA or multiple-splice variants. Since individual siRNA dosage can be reduced, off-target effects are minimized while maintaining specific gene suppression (27).

To overcome issues of gene compensation that would mask the effect of an isotype-specific siRNA pool, genes were chosen that had two or fewer known gene isotypes or variants of overlapping function. The exception was Rab5a, -b, and -c, for which all three isoform-specific siRNAs were used in the screen. Other gene variants, such as dynamins 1, 2, and 3 and WASF1, -2, and -3, have distinct functions in different cellular compartments and for this reason were also included (23, 51). The 79 targeted genes (excluding the control set) are listed in Table 1.

Reverse transfection and optimization of siRNA delivery. To optimize siRNA transfection of HeLa cells, a VSV-G-pseudotyped lentivirus expression vector was used initially to generate a population of cells with stable firefly luciferase expression. These cells were then transfected with various doses of DharmaFECT 1 transfection reagent (Dharmacon) together with siRNA-targeting luciferase or a nontargeting siRNA. From this preliminary work, conditions were identified (indicated below) that produced consistent suppression of 95% of luciferase activity in HeLa cells without noticeable cell toxicity. The siRNA suppression was evident 1 day after transfection and peaked on day 2, reaching a plateau that lasted until day 4, after which it subsided (not shown). Therefore, cells were infected with virus 2 days after transfection and infection was measured on day 3.

All transfections were performed in a 96-well format. A 1.6% (vol/vol) stock of

TABLE 1. List of genes targeted by siRNA pools used in this study[a]

Primary function and name of gene	GenBank accession no.[b]	OMIM no.[c]	Product name, function(s) and other characteristics[c]
Clathrin-mediated endocytosis			
AP1B1	NM_001127	600157	Beta prime subunit of the AP-1 clathrin-associated adaptor protein complex 1, important in the formation of clathrin-coated vesicles; present in late-Golgi/trans-Golgi network and endosomes
AP1M1	NM_032493	603535	Mu subunit of the AP-1 assembly complex
AP1M2	NM_005498	607309	Component of the AP-1 complex involved in basolateral sorting of endosomal cargoes
AP2A1	NM_014203	601026	Alpha subunit of clathrin-assembly complex 2 on endocytic vesicles; links receptors to clathrin
AP2A2	NM_012305	607024	Variant of above
AP2B1	NM_001030006	601025	Beta subunit of the clathrin assembly complex 2
CLTA	M20471	118960	Clathrin light chain A; major structural component of clathrin; one of two major classes of light chain (A and B)
CLTB	M20469	118970	Clathrin light chain B; major structural component of clathrin; one of two major classes of light chain (A and B)
CLTC	NM_004859	118955	Clathrin heavy chain; binds to light chain to form the clathrin triskelion
EPN4	NM_014666	607265	Epsin 4; stimulates clathrin assembly and binds clathrin
Eps15L1	NM_021235	See Eps15 600051	Eps15-like protein 1; may be involved in the internalization of ligand-inducible receptors of the receptor tyrosine kinase (RTK) type
ITSN1	AF064244	602442	Intersectin-1; adapter protein that may link clathrin-associated endocytosis of receptors to actin assembly machinery
ITSN2	AF182198	604464	As above
Caveolin-mediated endocytosis			
CAV2	AF035752	601048	Caveolin-2; coats the cytoplasmic face of caveolae; expressed in many cell types
CAV3	AF043101	601253	Caveolin-3; expressed predominantly in muscle but also in cells in culture
FYN	M14333	137025	Tyrosine kinase that may couple receptor signaling to caveolin and clathrin function
General endocytosis			
ARF1	M36340	103180	ADP ribosylation factor 1; involved in protein trafficking among different compartments; modulates COP1 function in vesicle budding and uncoating within the Golgi complex
DNM1	L07807	602377	Dynamin-1; highly expressed in the brain; involved in pinching off of endocytic vesicles from the plasma membrane
DNM2	L36983	602378	Dynamin-2; functions as above and also in actin cytoskeleton rearrangement; expressed broadly, highly expressed in muscle
DNM3	AB020627	See DNM-1	Dynamin-3; as above; may also have special functions in specific endocytic pathways
EEA1	L40157	605070	Early endosome antigen 1; binds Rab5 and early endosomal membranes
NEDD4	NM_006154	602278	Neural precursor cell expressed, developmentally downregulated; involved in ubiquitination of receptors prior to endocytosis
NEDD4L	NM_015277	606384	NEDD4-like; shares a ubiquitin ligase domain; as above
Rab5a	M28215	179512	RAS-associated protein 5A; required and rate limiting for early endosome formation
Rab5b	X54871	179514	Closely related to Rab5a; as above
Rab5c	U18420	604307	As above
Rab7B	NM_177403.3	Not available	RAS associated protein 7B; lysosome associated
SNAP91	NM_014841	607923	Synaptosome-associated protein of 91 kDa; similar to clathrin assembly protein AP180
Exocytosis			
Rab4A	M28211	179511	RAS-associated protein 4A; involved in recycling of endocytic vesicles from the early endosome to the cell surface
Rab4B	AF165522	See above	Variant of Rab4A

Continued on facing page

TABLE 1—*Continued*

Primary function and name of gene	GenBank accession no.[b]	OMIM no.[c]	Product name, function(s) and other characteristics[c]
Rab11A	X53143	605570	RAS-associated protein 11A; recycling endosomes to surface and trans-Golgi to surface
Rab11B	X79780	604198	Variant of Rab11A; as above
Rab11FIP5	NM_015470	See 608738	Rab11 family-interacting protein 5; rab11-regulating protein
Cytoskeleton and membrane remodeling, including actin rearrangement			
ARFIP2	NM_012402	601638	ADP ribosylation factor-interacting protein 2; binds directly to RAC1 and ARF proteins; modulates membrane ruffling
CAMK1	L41816	604998	Calcium/calmodulin-dependent protein kinase 1; involved in numerous cellular processes, including transcriptional regulation, hormone production, translational regulation, regulation of actin filament organization, and neurite outgrowth
CFL1	NM_005507	601442	Cofilin; reversibly controls actin polymerization and depolymerization; stimulated by phosphorylation by LIMK1
DAB2	NM_001343	601236	Disabled homolog 2; binds and stimulates GRB2 (see below)
GIT1	AF124490	608434	G protein-coupled receptor kinase-interacting protein 1; associated with and modulates signaling modules controlling vesicle trafficking, adhesion, and cytoskeletal organization
GRB2	NM_002086	108355	Growth factor receptor-bound protein 2; couples receptor signaling (including those for growth factors) to Rac-actin-modeling pathway
LIMK1	D26309	601329	LIM kinase domain 1; effector of Rho-induced actin polymerization/depolymerization by phosphorylation of cofilin
PACSIN1	AF242529	606512	Protein kinase C and casein kinase substrate 1 in neurons; may play a role in vesicle formation and transport; high expression in brain
PACSIN3	AF130979	606513	Protein kinase C and casein kinase substrate 3 in neurons; binds proteins important in vesicle trafficking, including dynamin 1, synaptojanin, synapsin 1, and N-WASP; ubiquitously expressed
PAK1	BC050377	602590	p21/CDC42/RAC1-activated kinase 1; activity results in depolymerization of F-actin; also acts on Jun N-terminal protein kinase 1 pathway; substrate of Rac1 and CDC42
RhoA	X05026	165930	RAS homolog gene family member A; involved in triggering actin cytoskeleton rearrangement
TNIK	AF172264	610005	TRAF2 and NCK interacting kinase; stress-activated serine/threonine kinase promotes actin depolymerization
ARP2/3 complex involved in nucleating actin polymerization			
ACTR2	NM_005722	604221	Actin-related protein 2; component of the ARP2/3 complex that promotes actin polymerization in lamellipodia
ACTR3	NM_005721	604222	Actin-related protein 3; one of the seven proteins that comprise the ARP2/3 complex; see ACTR2
ARPC1B	NM_005720	604223	Actin-related protein 2/3 complex subunit 1b; see ACTR2
ARPC2	NM_152862	604224	Actin related protein 2/3 complex subunit 2; see ACTR2
ARPC3	NM_005719	604225	Actin-related protein 2/3 complex subunit 3; see ACTR2
ARPC4	NM_005718	604226	Actin-related protein 2/3 complex subunit 4; see ACTR2
ARPC5	NM_005717	604227	Actin-related protein 2/3 complex subunit 5; see ACTR2
DDEF2	AB007860	603817	Development and differentiation-enhancing factor 2; regulates the formation of post-Golgi vesicles and modulates constitutive secretion and phagocytosis; modulates ARF1 and -5
PIP5K1A	U78576	603275	Phosphatidylinositol-4-phosphate 5-kinase 1A; involved in actin cytoskeleton modulation
ROCK1	U43195	601702	Rho-associated coiled-coil-containing protein kinase 1; downstream effector of RhoA, phosphorylating LIMK1 to regulate the actin cytoskeleton
ROCK2	D87931	604002	Rho-associated coiled-coil-containing protein kinase 2; isozyme of ROCK1; see ROCK1

Continued on following page

TABLE 1—*Continued*

Primary function and name of gene	GenBank accession no.[b]	OMIM no.[c]	Product name, function(s) and other characteristics[c]
WASF1	AF134303	605035	Wiskott-Aldrich syndrome protein family member 1; (WAVE1); transmits signals from tyrosine kinase receptors and small GTPases to the actin cytoskeleton; involved in filopodium formation; effector of RAC1
WASF2	AB026542	605875	Wiskott-Aldrich syndrome protein family member 2; homolog of WASF1
WASF3	AB026543	605068	Wiskott-Aldrich syndrome protein family member 3; homolog of WASF1
Others			
ARRB1	NM_004041	107940	β-Arrestin 1; targets receptors to clathrin-coated vesicles; binds SRC
ARRB2	NM_004313	107941	β-Arrestin 2; homolog of ARRB1; promotes receptor internalization
ATM	U33841	607585	Ataxia-telangiectasia mutated gene; checkpoint control in DNA repair; may play a role in vesicle and/or protein transport by binding beta adaptin
ATP6V0A1	NM_005177	192130	ATPase, H^+ transporting, lysosomal V0 subunit A1; component of the vacuolar ATPase proton pump involved in endosomal acidification
BIN1	AF004015	601248	Bridging interactor 1; binds integrins; associated with CAV3 in muscle
CBL	NM_005188	165360	CAS-BR-M murine ecotropic retroviral-transforming sequence homolog; regulates receptor tyrosine kinase degradation and possibly endocytosis through ubiquitination
CBLB	NM_170662	604491	CAS-BR-M murine ecotropic retroviral-transforming sequence B; related to CBL
CBLC	NM_012116	608453	CAS-BR-M murine ecotropic retroviral-transforming sequence C; interacts with PI3K, FYN, and GRB2; may alter EGFR endocytosis
GORASP1	NM_031899	606867	Golgi reassembly stacking protein-1; Golgi structural protein
IHPK3	NM_054111	606993	Inositol hexaphosphate kinase 3; may regulate inositol phosphate-stimulated vesicle formation and trafficking
MAP4K2	U07349	603166	Mitogen-activated protein kinase 2; associated with Rab8 and may control protein secretion
MAPK8IP1	NM_005456	604641	Mitogen-activated protein kinase 8-interacting protein 1; accumulates in cell surface projections and interacts with proteins affecting the Jun N-terminal kinase pathway
MAPK8IP2	NM_012324	607755	Mitogen-activated protein kinase 8-interacting protein 2; as above
MAPK8IP3	NM_015133	605431	Mitogen-activated protein kinase 8-interacting protein 3; as above; binds kinesin; acts as a molecular scaffold for Jun N-terminal kinase pathway proteins
PSCD3	NM_004227	605081	Pleckstrin homology, SEC7, and coiled-coil domain protein 3; regulates ARF proteins to control vesicle trafficking
STAU	NM_004602	601706	Staufen homolog; cross-links cytoskeleton and RNA
SYNJ1	NM_003895	604297	Synaptojanin 1; binds Eps15 and is localized to clathrin-coated vesicles; high levels in neurons
SYNJ2	NM_003898	609410	Synaptohanin 2; ubiquitously expressed; effector or RAC1 in actin regulation and lamellipodium formation and clathrin-mediated endocytosis
SYT1	M55047	185605	Synaptotagmin 1; important in exocytosis and endocytosis in neurons
SYT2	NM_177402	600104	Synaptotagmin 1; as above

[a] These are a subset of the Dharmacon Membrane Trafficking siRNA library. Each is ordered by reported primary function and then alphabetically.
[b] GenBank database 2006 (http://www.ncbi.nlm.nih.gov/).
[c] The description of gene function is summarized from Online Mendelian Inheritance in Man (OMIM), McKusick-Nathans Institute for Genetic Medicine, Johns Hopkins University (Baltimore, MD), and National Center for Biotechnology Information, National Library of Medicine (Bethesda, MD), as of October 2006. http://www.ncbi.nlm.nih.gov/omim/.

DharmaFECT 1 transfection reagent was made in Dharmafect cell culture reagent (Dharmacon) and incubated for 10 min. From this stock, 25 μl was added to the lyophilized siRNA in each well and incubated at room temperature for 30 min to allow the siRNAs to rehydrate and form siRNA-lipid complexes. Then, 10^4 cells in 100 μl of complete Dulbecco's modified Eagle's medium supplemented with 10% fetal bovine serum was added and the medium was changed after 24 h. The final concentration of pooled siRNAs per well was 6.25 pmol. Individual siRNA duplexes were also used at 6.25 pmol per well.

Screening of the siRNA library. For screening, recombinant RSV that expressed GFP as a marker of infection was used (61). After HeLa cells were transfected with siRNA, virus was introduced at an MOI of 0.05. GFP expression was evident at 20 h postinfection, at which time monolayers were photographed

(4 images per well) using a 10× lens objective. The impact of each siRNA on virus infection was analyzed by counting the cells expressing GFP. The controls included in each experiment were the use of transfection reagent alone, a nontargeting siRNA (Dharmacon), a red fluorescent nonspecific siRNA (siGLO, Dharmacon), and siRNA pools targeting glyceraldehyde-3-phosphate dehydrogenase or lamin A/C. The *kif11* gene product is required for cell survival, and siRNAs targeting this gene are cytotoxic. Therefore, *kif11* siRNA provided a measure of siRNA efficacy by measuring cell death. The other siRNAs served as negative controls for nonspecific effects of siRNA and/or the transfection reagents on cell viability and virus infection. For screening, the number of infected cells for each siRNA treatment was normalized to the average number of infected cells for the negative-control siRNAs. In all cases, cell viability was checked by visually inspecting cells using phase-contrast microscopy.

Use of dominant-negative forms of endocytic-trafficking mediators and virus challenge. Plasmids encoding wild-type, dominant-negative, or constitutively active mutant forms of proteins important in endosomal trafficking were cloned into the mammalian expression plasmid pLENTI6 (Invitrogen). Each gene was tagged with GFP and has been characterized elsewhere (30). The mutant genes included Eps15 Δ95–295 (a component of the AP2 clathrin adapter complex; the dominant-negative form inhibits clathrin-coated pit budding); Rab5 S34N (a dominant-negative form that inhibits early endosome formation); and Rab5 Q79L (a constitutively active Rab5 that drives the formation of enlarged early endosomes). To control for the effects of GFP expression on infection, a GFP-expressing plasmid was used.

Each expression construct was transfected into HeLa cells, at 20% confluence, using calcium phosphate. After overnight incubation, the medium was replaced. RSV, VSV or recombinant 10A1 MLV were added to cells 36 h after transfection and incubated with cells for 1 h. Unbound virus was removed by replacing the medium twice. RSV-infected cells were incubated for 20 h, VSV-challenged cells were incubated for 7 h, and 10A1 MLV-infected cells were incubated for 36 h before detection of virus infection.

Cell surface staining for detection of virus infection by FACS. Virus infection of cells was detected by FACS analysis after staining cells for the expression of virus-specific envelope proteins or CD4.1 infection reporter for 10A1 MLV. The cells were washed twice in phosphate-buffered saline (PBS) and detached from the plate with 5 mM EDTA in PBS. The cells were fixed in freshly made 4% (wt/vol) paraformaldehyde (buffered to pH 7.4 with PBS) for 5 min, then washed in PBS and incubated for 30 min in PBS supplemented with 1% bovine serum albumin to block nonspecific binding of antibodies. All incubations with antibodies were performed in PBS and 1% bovine serum albumin. For RSV and VSV, cells were incubated for 1 h with virus-specific antibody at a 1:200 dilution, and then washed three times and incubated for 30 min with secondary Alexa $Fluor_{647}$-labeled anti-mouse immunoglobulin G (Invitrogen) at a 1:500 dilution. For the recombinant 10A1 MLV, cells were directly stained with an anti-CD4 Alexa $Fluor_{647}$ conjugate (Becton Dickinson, NJ) as recommended by the manufacturer. The cells were washed three times and analyzed by using a FACS.

FACS analysis. Stained cells were analyzed on a FACSCanto instrument (Becton Dickinson). At least three independent experiments were performed, and at least 5×10^4 cells were sampled each time. The cells were gated based on forward and side light scatter to ensure the inclusion of individual cells only, without any debris or aggregates. To analyze the impact of recombinant gene expression, cells were gated by the expression level of the GFP-tagged gene, using a 488-nm laser as an excitation source. The transfection conditions were optimized to give approximately 20% of cells expressing the GFP-tagged protein at moderate to high levels. The cells were stained as described above to detect virus infection and then scanned with a 633-nm laser. As a control for cellular autofluorescence, HeLa cells were transfected with a plasmid vector encoding β-galactosidase. As a control for the contribution of debris in the virus inoculum and for nonspecific antibody binding to cells, infected cells were stained prior to the expression of virus envelope proteins (3, 6, or 12 h after infection with VSV, RSV, or recombinant 10A1 MLV, respectively). The use of the two different lasers (488 and 633 nm) for the excitation of fluors prevented problems of signal contamination from one fluorescence channel into the next. All data were analyzed by using FlowJo 7.1 software from Tree Star Inc. (Ashland, OR).

Counting of cell-bound virus particles. The binding of virus to cells was optimized to permit the visualization of distinct punctate staining on the cell surface. Virus was concentrated by pelleting through 20% sucrose in 20 mM HEPES, pH 7.4. The concentrated virus was then bound to cells by incubation for 2 h at 4°C to prevent cellular endocytosis. The cells were then washed twice in ice-cold PBS and fixed in paraformaldehyde as described above for FACS experiments. The cells were then stained with anti-RSV F antiserum (1:200 dilution), followed by Alexa $Fluor_{594}$-labeled secondary antibody (1:200 dilution). Confocal microscopy was performed using a Zeiss LSM 510 META laser-scanning confocal microscope. At an MOI of 10, distinct virus particles were visible. To count the virus particles bound to cells, uncompressed TIF images were analyzed by the Wright Cell Imaging Facility (WCIF) version of the ImageJ software package (http://www.uhnresearch.ca/facilities/wcif/imagej/). Counting of virus particles was performed on a cell-to-cell basis using the "analyze particles" function and was normalized to the total area of the cell. The margins of each cell were defined manually by referring to matched visible light phase-contrast images and using the "region of interest" function of the software.

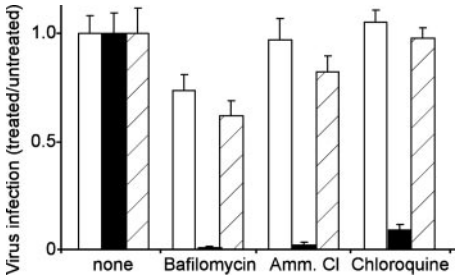

FIG. 1. RSV infection is insensitive to lysosomotropic agents. HeLa cells were treated with bafilomycin A1 (10 nM), ammonium chloride (Amm. Cl.; 10 mM), or chloroquine (10 μM) for 1 h prior to the addition of virus. RSV (open bars), VSV-G-pseudotyped MLV (solid bars) or ecotropic MLV envelope protein-pseudotyped MLV (diagonal striped bars) were then added (MOI, 0.1) to the cells and incubated for an additional 5 h in the presence of each drug. The medium was then replaced, and the infected cells were counted after 20 h for RSV or 36 h for ecotropic MLV envelope protein- or VSV-G-pseudotyped viruses. Each virus encoded GFP as an infection marker. The means ± SDs of the results of three independent experiments are shown.

Statistics. Statistical analysis was performed using GraphPad Prism version 4.00 for Windows (GraphPad Software, San Diego, CA). Data were compared by one-way analysis of variance, and analysis included the Tukey-Kramer posttest.

RESULTS

RSV infects HeLa cells through a pH-independent mechanism. It was reported that infection of HEp-2 cells with RSV resisted treatment with the lysosomotropic agent ammonium chloride (48). In the current studies, we used HeLa cells, since these cells are susceptible to RSV, are readily transfected with siRNA, and have been extensively studied for endocytic trafficking. Since the infection route can be cell type dependent, the effects of lysosomotropic agents on infection of the HeLa cells were tested. Cells were incubated with virus in the presence of ammonium chloride, chloroquine, or bafilomycin A1. The latter is a specific inhibitor of the vacuolar ATPase that is required for the acidification of endosomes, while ammonium chloride and chloroquine buffer against the endosomal pH gradient. Consistent with previous observations in HEp-2 cells, RSV infection was unaffected by ammonium chloride (Fig. 1). Similarly, infection was unaffected by chloroquine and only partially inhibited by bafilomycin (which was attributed to drug toxicity). In each case, RSV behaved like ecotropic MLV, which has similarly been shown to be a pH-independent virus (30). In contrast, VSV infection was blocked by >90% with each drug. These findings indicated that the RSV infection of HeLa cells is comparable to that of ecotropic MLV, as it does not require endosomal acidification for infection.

Choice of siRNA library. The lack of pH sensitivity of RSV suggested that endocytosis was not required for infection. Instead, RSV may rely more on actin-dependent trafficking after

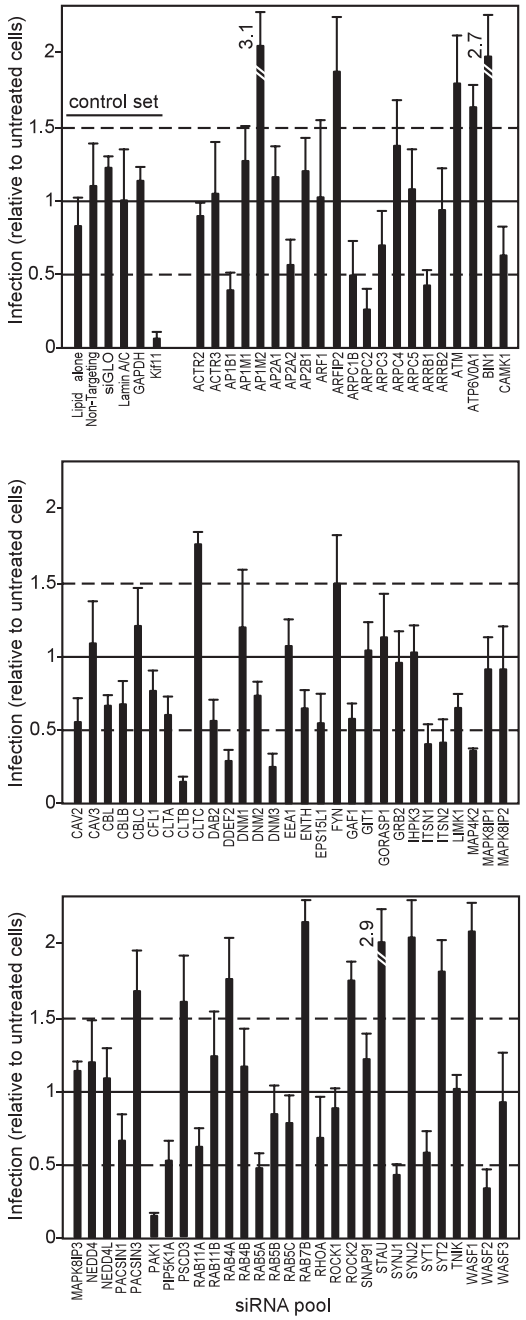

FIG. 2. The impacts of siRNAs targeting genes important in endocytosis and cytoskeleton rearrangement on RSV infection. HeLa cells were transfected with siRNAs and, after 2 days, the cells were infected with recombinant RSV encoding GFP at an MOI of 0.05. Twenty hours postinfection, the infected cells expressing GFP were counted. To establish a baseline of infection and transfection efficiency, cells were treated with a control set (top right) of siRNAs and/or transfection reagent, which included transfection lipids alone or together with "nontargeting" siGLO (fluorescently labeled) nonspecific siRNA or siRNAs targeting lamin A/C or glyceraldehyde-3-phosphate dehydrogenase. *kif11* is required for cell survival, and siRNA targeting this gene rapidly kills cells. Together with the siGLO siRNA, the *kif11* siRNA permitted monitoring of transfection efficiency. In all experiments, >90% of cells became fluorescent or died after treatment with siGLO or Kif11, respectively, indicating a high transfection efficiency and siRNA suppression of Kif11. The cells were then treated with siRNA pools targeting each of the indicated genes (total of 79). The cells were infected (as above), and the levels of infection monitored by GFP expression. The infection efficiencies were normalized to the average number of infected cells after treatment with the control set (except for Kif11). Dashed lines indicate the threshold used in the assay (two times the average SD of the data). The averages ± 1 SD of the results of three independent experiments are shown. Accession numbers and a brief description of the role of each gene are provided in Table 1.

entry at the cell surface, as observed for vaccinia virus (44). siRNA gene-silencing technology was used to test this concept. An array of 79 siRNA pools targeting genes known to be directly or indirectly involved in controlling the polymerization of actin, cytoskeleton rearrangement, endocytosis, and vesicle/cargo movement was used to identify host genes necessary for RSV infection. A list of the targeted genes and a brief description of the reported role for each are provided in Table 1.

siRNA screen indicates that clathrin-mediated endocytosis is required for RSV infection. By setting the threshold of significance of the screen to two times the average standard deviation (SD) of all the infection data (slightly less than a twofold change in infection), three categories of siRNA-induced effects were observed: (i) those that suppressed infection, (ii) those that elevated infection, and (iii) those having no effect on infection (Fig. 2). Surprisingly, the siRNAs that gave the strongest inhibition of infection were those that targeted genes involved in endocytosis. These included clathrin light chain (CLTB; 80%), the beta-prime subunit of the clathrin adapter complex 1 (AP1B1; 60%), dynamin 3 (DNM3; 75%), and Rab5A (52%). The clathrin light and heavy chains together form the triskelion coat that distinguishes clathrin-coated pits from other endosomes. AP1B1 is part of the AP1 complex important in regulating clathrin-coated pit formation and targeting receptors to coated pits. Dynamin 3 is required for the release of clathrin-coated and other vesicle types from the plasma membrane by inducing membrane scission, and Rab5 isoforms are required for early endosome formation.

Three siRNAs that targeted genes encoding proteins important for modulating receptor function by endocytosis (20, 40) were also potent inhibitors of RSV infection. These were β-arrestin 1 (ARRB1; 60%) and intersectins 1 and 2 (ITSN1 and -2; both gave 60% inhibition of infection). Intersectins may couple proteins attached to clathrin-coated vesicles to actin, which provides the driving force in vesicular transport (26). Genes important in regulating actin polymerization were also indicated. These were PAK1 and WASF2. PAK1 is a substrate of the GTPases Rac1 and CDC42 and, once activated, stimulates F-actin depolymerization (15). WASF2 is also an effector of Rac1 and is important in the regulation of cytoskeleton assembly (51).

The greater than twofold increases in infection seen after treatment with some siRNAs (which included siRNAs targeting Stau, Bin1, and AP1M2) were unexpected. Stau is involved in RNA association with the cytoskeleton and could be important for subcellular localization of the viral genome. Bin1 (amphiphysin 2) isoforms are involved in numerous processes, including endocytosis and cell cycle regulation (58). AP1M2 (the siRNA raised the level of infection by more than threefold) is implicated in the regulation of clathrin-mediated en-

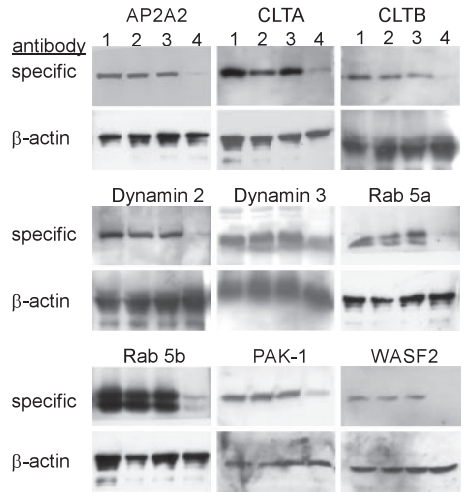

FIG. 3. Confirmation of siRNA suppression of protein expression. Where antibodies could be obtained and were of sufficient sensitivity to detect endogenous protein, Western blots were performed after treatment with siRNAs (as indicated above the blots). For each experiment, cell lysates were made from untreated cells (lane 1), cells treated with transfection reagent alone (lane 2), cells treated with transfection reagent together with nontargeting siRNA (lane 3), or transfection reagent with siRNA targeting the indicated gene (lane 4). The lysates were made 2 days after siRNA transfection in sodium dodecyl sulfate-polyacrylamide gel electrophoresis loading buffer with 2% β-mercaptoethanol. After samples were boiled for 5 min, each was loaded on 10 or 12% polyacrylamide gel electrophoresis gels as appropriate and transferred to nitrocellulose membranes and the blots were stained with each specific antibody (upper panels). The blots were then destained and reprobed with β-actin-specific antibody which served as a gel-loading control (lower panels).

docytosis that targets receptors to the basolateral membrane of polarized cells (17). The mechanisms of the siRNA-induced increases in infection could be explained if each gene is normally involved in suppressing virus infection directly or misdirects virus into pathways that are nonproductive.

In each of these experiments, the general cytotoxicity was minimal, with only *kif11*- (cytotoxic siRNA control) and cofilin (CFL1)-targeting siRNAs showing >90% and 40% cell loss, respectively. All other siRNAs did not affect cell viability sufficiently to contribute to the outcome of the screen. Overall, the screen indicated an unexpected but strong role for clathrin-mediated endocytosis in RSV infection, which was investigated further.

The findings from the initial screen were first validated by separately testing the activities of individual siRNAs from each pool. It was expected that the observed effect was specific for the targeted gene and not due to off-target gene suppression if two or more distinct siRNAs targeting the same gene similarly affected infection (27). Since pools can sometimes be less efficient at suppressing particular genes, those pools that gave a weak suppression (between 50 and 60%) of RSV infection were also tested as individual siRNAs. Genes targeted by two or more siRNAs giving a significant ($P < 0.05$) reduction in virus infection are listed in Table 2. For each of the clathrin-associated genes discussed above, at least two siRNAs also inhibited infection, and these included siRNAs against clathrin light chain B and the components of the clathrin adapter complexes AP1 and AP2. Some strong hits from the primary screen were not supported by the duplex screen, including ARRB1, DDEF2, and ITSN1. In contrast, some weakly suppressing (50 to 60% inhibition of infection) pools of siRNAs gave two or

TABLE 2. Genes targeted by more than two distinct siRNAs suppressing RSV infection

Gene and primary function[a]	Number of siRNAs giving significant ($P < 0.05$)[b] reduction	Reported function and other characteristic(s) of product
Clathrin-coated pit formation		
AP1B1	3	Subunit of clathrin-associated adaptor protein complex 1
AP2A2	2	Subunit of clathrin-associated adaptor protein complex 2
CLTB	2	Clathrin light chain B subunit; required for clathrin-coated pits
DAB2	2	Adapter protein that couples receptors into clathrin-coated pits
ITSN2	3	Regulates formation of clathrin-coated vesicles
SYNJ1	2	Localized to clathrin-coated vesicles and binds EPS15
Endocytosis		
DNM3	2	Dynamin 3; required for pinching off endocytic vesicles from the plasma membrane
RAB5A	3	Required for early endosome formation
RAB5B	3	As for Rab5A
RAB5C	2	As for Rab5A
GAF1	2	RAB11-interacting protein
RAB11A	2	Important in recycling endosomes
SYT1	2	Involved in endocytosis
Actin polymerization		
ARPC1B	3	Part of the ARP2/3 complex implicated in the control of actin polymerization
PAK1	2	Regulates actin through Rac1
WASF2	2	Involved in signaling through actin

[a] The genes listed are those targeted by two or more single-siRNA duplexes that suppressed RSV infection signficantly ($P < 0.05$) at a dosage of 6 pmol per well of a 96-well plate containing 10^4 cells.

[b] Statistical significance was determined by one-way analysis of variance using the Tukey-Kramer posttest at a 95% confidence interval. The experiment was repeated twice, with similar outcomes.

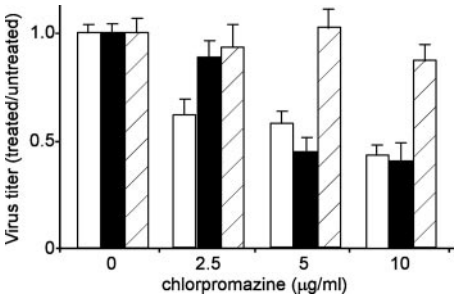

FIG. 4. Chlorpromazine inhibits infection by RSV. The clathrin endocytosis inhibitor, chlorpromazine, was used at the indicated dosages to confirm that RSV required clathrin-mediated endocytosis for infection. Cells were treated following the same regimen as described in the Fig. 1 legend, with 1 h of pretreatment of cells and removal of the drug 5 h after the addition of virus. The cells were infected with recombinant RSV encoding red fluorescent protein (open bars) or with a VSV-G (solid bars) or 10A1 MLV (bars with diagonal stripes) envelope protein-pseudotyped retrovirus encoding GFP. Infected cells were counted by microscopy and the results were normalized to those for the untreated control for each virus. The means ± 1 SD of the results of three replicate experiments are shown.

more siRNA duplexes that significantly inhibited infection, including AP2A2, DAB2, GAF1, and RAB11A. The confirmed hits from this screen were then investigated further.

Confirmation of suppression of protein expression by Western blotting. Western blots were used to confirm that siRNA treatment suppressed expression of the targeted genes (Fig. 3). Cells treated with AP-2 alpha2, clathrin light chain B, dynamin 3, *rab5a* or *-5b*, PAK-1, and WASF2 siRNAs showed dramatic reductions in the levels of the respective proteins (72 to 98% as measured by densitometry) compared to the levels in untreated or mock-treated (nonspecific antibody) cells. This work indicated a strong correlation between the impact of each siRNA on RSV infection and the suppression of protein expression. Unfortunately, the effects of siRNA on the expression patterns of the remaining genes listed in Table 2 could not be confirmed due to the lack of reagents sensitive enough to detect the presence of endogenous proteins, even when a 10-fold excess of cell lysates was loaded on the gel. To demonstrate that a specific class of clathrin, dynamin, and Rab5 was important for infection, Western blots were performed after treatment with siRNAs against variants and isoforms of the above set of genes. For clathrin light chain A, dynamin 2, and Rab5B, it was found that cells expressed detectable amounts of these proteins and the siRNAs specifically and similarly reduced the expression of each. Interestingly, this part of the work highlighted a greater need for specific subsets of proteins involved in endocytosis over other closely related proteins of similar function.

Chlorpromazine inhibits RSV infection. To confirm the role of clathrin-mediated endocytosis in RSV infection, cells were treated with chlorpromazine, a drug that specifically inhibits this endocytic pathway (57), and then challenged with virus (Fig. 4). Surprisingly, RSV was more sensitive to this drug treatment than VSV, being significantly inhibited at 2.5 μg/ml of the drug ($P < 0.01$), while VSV was not significantly affected ($P > 0.05$). At higher concentrations, both VSV and RSV were significantly inhibited, by more than 50% each ($P < 0.001$), a level seen for pH-dependent viruses (7). In contrast, the 10A1 MLV control was not affected by any of the doses used ($P > 0.05$).

Expression of dominant-negative mutants confirms role of clathrin-mediated endocytosis. To further test the role of clathrin-mediated endocytosis in RSV infection, cells expressing GFP-tagged mutant forms of Eps15 and Rab5 (proteins required for clathrin-mediated endocytosis and endosome formation, respectively) were challenged with RSV, VSV, or 10A1 MLV. VSV is reported to require clathrin-dependent endocytosis for infection (30) and served as a control to show disruption of endocytosis. Conversely, 10A1 MLV is a pH-independent virus that does not require clathrin-mediated endocytosis for infection (7). For VSV and RSV, virus infection was monitored by the detection of viral envelope protein expression and expression of the recombinant gene was detected by GFP fluorescence using FACS analysis (Fig. 5A). For 10A1 MLV, a recombinant virus encoding a truncated form of CD4 as a marker of infection was used and also analyzed by FACS. The impact of the expression of each gene on infection was determined by calculating the change in the level of infection when levels in cells expressing the recombinant GFP-tagged protein that affected endocytosis were compared to the level in cells expressing GFP alone (Fig. 5B). In this way, the infection levels and recombinant gene expression could be precisely correlated.

Eps15 is a well-characterized protein required for clathrin-mediated endocytosis through interaction with the AP-2 complex (5), and the dominant-negative form, Eps15 Δ95–295, potently inhibits the formation of clathrin-coated endosomes (6). The overexpression of Eps15 Δ95–295 greatly reduced the levels of both VSV and RSV infection compared to that of the GFP control (76% and 68% reduction, respectively, $P < 0.001$), while the level of 10A1 MLV infection was slightly elevated. As noted by others, the expression of this gene was faint, even though it was functional (12), and not as many cells expressing the gene were gated for analysis as for our later gene expression work, described below. However, adjusting the gates to the left to compensate for the low expression signal did not alter the outcome or significance of the analysis, even though the number of cells included increased. The effect of the dominant-negative gene was specific and not due to the GFP tag, since the levels of infection of cells expressing GFP alone were not different from the levels in nontransfected cells. The unaffected 10A1 MLV infection level also indicated that the effect was not due to general toxicity. For those cells that escaped transfection or expressed low levels of the transgene, the frequencies of infected cells were similar to those of cells transfected with the β-galactosidase- or GFP-expressing control plasmids. This ratio served as an important internal control to which data could be normalized to account for any experiment-to-experiment variation (Fig. 5B). In conclusion, the effects of Eps15 Δ95–295 strongly supported a role for clathrin-mediated endocytosis in RSV infection.

To further substantiate the role for clathrin-mediated endocytosis in infection, the importance of Rab5, a protein required for early endosome formation, was evaluated. FACS analysis was used, with GFP-tagged forms of Rab5 transfected into

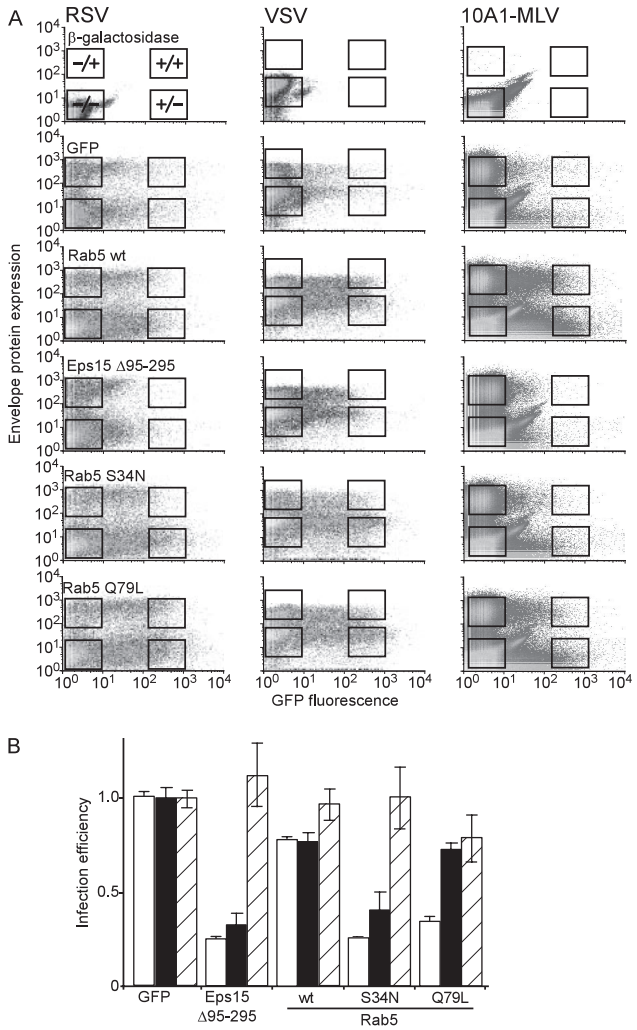

FIG. 5. FACS analysis indicates that clathrin-mediated endocytosis is important for RSV infection. Cells were transfected with plasmids encoding β-galactosidase, GFP, Eps15 Δ95–295, wild-type or dominant-negative Rab5 (S34N), or constitutively active Rab5 (Q79L). The Eps15 and Rab5 proteins were each tagged with GFP. After 2 days to allow peak expression, the cells were challenged with wild-type RSV, VSV, or recombinant 10A1 MLV (encoding a truncated CD4 as an infection marker), each at an MOI of 0.2. (A) Cells were stained with RSV- or VSV-specific antibodies followed by Alexa $Fluor_{647}$-labeled secondary antibody or with Alexa $Fluor_{647}$-labeled anti-CD4. The cells were then analyzed by using a FACS. After gating for single cells, at least 5×10^4 cells were analyzed. Cells transfected with β-galactosidase-encoding plasmids and stained prior to virus protein expression (3 h for VSV and 6 h for RSV or 20 h for 10A1 MLV) were used to define the autofluorescence levels. Cells expressing GFP alone were used to define the infection levels in normal cells. The gates for data analysis were uninfected cells expressing no GFP-tagged protein (indicated by −/− box), those not infected but expressing moderate to high levels of tagged protein (+/−), or those infected with virus and not expressing (−/+) or expressing tagged protein (+/+). The cells not expressing tagged protein served as important internal controls to monitor the levels of infection of normal cells compared to the levels in those expressing the recombinant protein. (B) The proportions of cells infected with VSV (open bars), RSV (solid bars), or 10A1 envelope protein-pseudotyped MLV (bars with diagonal lines) and expressing recombinant GFP-tagged protein were calculated by dividing the number of infected cells expressing tagged protein by the total number of cells expressing tagged protein. This value was then normalized to the proportion of infected cells not expressing GFP-tagged protein. The means ± 1 SD of the results of 3 independent experiments are given. wt, wild type.

cells which were then challenged with virus and stained as above. Both dominant-negative and constitutively active forms of Rab5 were used. The overexpression of wild-type Rab5 reduced VSV and RSV infection levels to a small but significant extent (20%; $P < 0.001$), consistent with the reported observation that Rab5 overexpression can alter endocytosis by increasing receptor (with attached virus) recycling back to the cell surface (50). In contrast, the dominant-negative S34N mutant form of Rab5 had a more-dramatic effect, reducing the levels of infection of both VSV and RSV by 75 and 60%, respectively (Fig. 5). Statistical analysis indicated that the infection levels for both viruses were significantly reduced compared to the levels for both GFP-expressing and wild-type-Rab5-expressing cells ($P < 0.001$). For 10A1 MLV, the levels of infection were unaffected by either wild-type Rab5 or the S34N mutant. Interestingly, the behavior of VSV and RSV differed in cells expressing the constitutively active Rab5 Q79L mutant which drives the formation of large early endosomes and inhibits the progression to the late endosome. Whereas VSV infection was significantly inhibited (66%) compared to that in GFP- or wild-type-Rab5-expressing cells ($P < 0.001$), the level of RSV infection (reduced by 28%) was not significantly different from that in wild-type-Rab5-expressing cells or the level of infection seen with 10A1 MLV ($P > 0.05$).

Since Rab5 overexpression might disrupt the envelope protein expression used to detect infection by FACS, the results were confirmed by using virus expressing red fluorescent protein detected with conventional microscopy. A similar pattern of inhibition of infection was seen. Cells expressing moderate to high levels of the dominant-negative mutants of Eps15 and Rab5 were less susceptible to infection by RSV, while those that expressed the constitutively active Rab5 were still infected (Fig. 6). Both the microscopy and FACS data strongly supported the finding from using siRNAs that endocytosis is required for RSV infection. Importantly, the behavior of RSV is closer to that of VSV than of 10A1 MLV. The exception was in the infection levels seen with cells expressing Rab5 Q79L and suggests an interesting difference in the endosomal requirements of each virus. Unlike VSV, RSV may not require early-to-late endosome maturation to infect cells, instead exiting the endosomal pathway soon after early endosome formation. Additional work will be required to confirm this finding.

A possible mechanism by which the dominant-negative Eps15 and Rab5 mutants might inhibit infection would be to down-regulate receptors from the cell surface. To rule out this possibility, binding assays were performed by incubating cells with wild-type RSV and labeling bound virus with anti-F-specific antibody (Fig. 7). Microscopy revealed similar amounts of labeled RSV particles bound to cells expressing GFP alone or GFP-tagged wild-type Rab5, Eps15 Δ95–295, Rab5 S34N, and Rab5 Q79L. While this result suggests that receptor down-regulation was not occurring, binding was observed to occur in clusters, suggesting that virus receptors may be segregated on the membrane. A focus of future experiments will be to determine if virus clusters at sites of clathrin-coated pit formation.

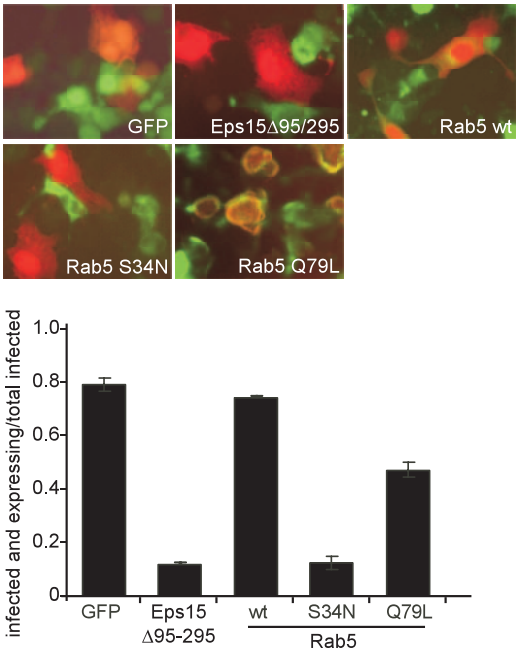

FIG. 6. Microscopy analysis confirms that RSV requires clathrin-mediated endocytosis for infection. Cells were transfected with plasmids carrying the indicated genes and challenged 2 days later with recombinant RSV encoding red fluorescent protein. After 30 h, the cells were photographed using a Leica DMIRB inverted fluorescence microscope detecting the green fluorescence of the GFP-tagged transfected gene and the red fluorescence of the RSV infection marker (upper panel). The impact of the expression of each gene was determined by counting the cells infected with RSV that were also expressing the GFP-tagged protein and dividing by the total number of infected cells (lower panel). The averages ± 1 SD of the results of three replicate experiments are shown. wt, wild type.

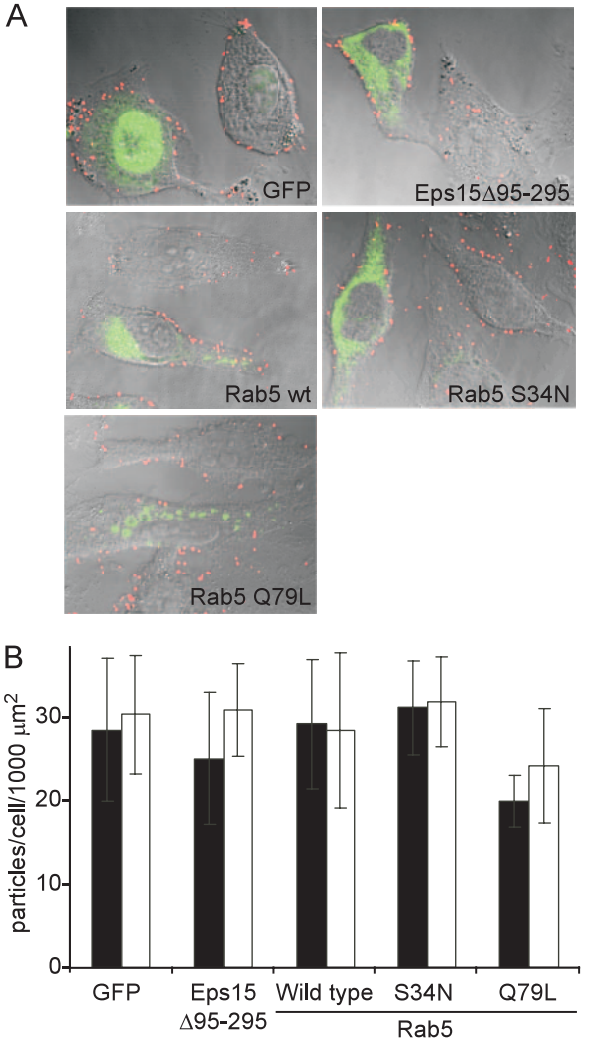

FIG. 7. Expression of Eps15 or Rab5 proteins does not alter virus binding to cells. Cells were transfected with expression plasmids carrying the indicated genes. Each gene product was GFP tagged. (A) Virus was then added to the cells on ice and incubated for 2 h, after which excess virus was removed by washing and pelleting cells in ice-cold PBS. The cells were then fixed and stained as detailed in Materials and Methods. The cells were then photographed using a Zeiss LSM 510 confocal microscope, and the images analyzed using ImageJ software. Each image is a composite of the visible light phase-contrast image and the fluorescence images of GFP expression (green) and labeled virus (red). Midsections of cells expressing the GFP-tagged protein and untransfected cells in the same field are shown and virus is visible on the cell periphery. In some instances, the surface of the untransfected cell is in the focal plane and virus can be seen on the cell surface as well. wt, wild type. (B) For each cell population, the total number of labeled virus particles per cell was determined by counting using ImageJ software and was normalized to the cell area as described in Materials and Methods. At least five transfected and untransfected cells were used for each analysis. The average numbers of particles per cell ± 1 SD are shown.

DISCUSSION

We conclude that RSV is an enveloped virus that requires clathrin-mediated endocytosis but not endosomal acidification to infect cells. The studies established this observation with multiple corroborating experimental approaches, and concomitantly determined the value of targeted siRNA profiling to extend our understanding of viral pathogenesis. The concepts that are discussed may be relevant to other pH-independent viruses whose entry and productive infection requirements are not fully defined. Few other examples exist of pH-independent enveloped viruses that use endocytosis to efficiently infect cells. Human immunodeficiency virus (HIV) can inefficiently infect cells after being endocytosed (12), but entry still appears to occur predominantly at the cell surface (49). Until recent work was published, avian leucosis virus, a retrovirus afflicting birds, was also thought to enter at the cell surface because, as for other retroviruses, inhibitors of endosomal acidification did not block infection. It was not until a close scrutiny of infection kinetics that a pH-dependent step required after receptor engagement was revealed (14, 47). However, we do not believe that RSV is the same, since the parameters of infection were set to specifically detect any lag in infection due to effects of the lysosomotropic drug treatment. It is now important to determine if RSV is an exception or if other paramyxoviruses share this pathway of entry and require endocytosis before infection can take place. This knowledge will help in the development of better agents for the treatment of paramyxovirus infection.

Aside from pH, few other endosomal triggers of virus entry into cells have been identified. Even the recently reported cathepsin cleavage of the Ebola virus envelope protein, re-

quired before virus entry can take place, uses a pH-dependent protease (10). A few reports indicate that disulfide bond rearrangement may be important in HIV entry, but this is still believed to occur on the cell surface (18). Thus, pH insensitivity of a virus is often equated with lack of need for endocytosis. The ability to form syncytia at neutral pH is also considered to be a strong indicator of competence for entry at the plasma membrane. This demonstrates that the envelope proteins are capable of fusing cell and virus membranes at the cell surface, but it does not indicate if such fusion leads to a productive virus infection. RSV drives syncytium formation at neutral pH (48) and was shown to have a pH-insensitive infection mechanism in HEp-2 cells (48). We showed that the infection of HeLa cells was similarly unaffected by the endosomal acidification inhibitors ammonium chloride, chloroquine, and bafilomycin A1. Historically, these observations have been interpreted to mean that RSV entered at the cell surface.

Recently, it was reported that internalization of receptor-bound MLV (a pH-insensitive retrovirus that is thought to enter at the cell surface) may precede entry and this was likely to be actin and myosin dependent (31). We wanted to know if RSV showed a similar dependence on actin function. Indeed, RhoA activity, an activator of actin polymerization, was shown to be required for syncytium formation by RSV (21). Also, actin disruption using cytochalasin inhibited RSV uptake in dendritic cells (59). Unfortunately, these studies did not identify the actual role of actin in RSV infection itself. In the current work, actin-associated genes were identified as important for RSV infection but the identified genes were those predominantly associated with endocytosis.

Genes important in actin polymerization were ARRB1, ARPC2, DDEF2, PAK1 (also termed PAK-alpha), and WASF2 (WAVE2). Each is important in coupling clathrin-mediated endocytosis to actin. β-Arrestin (ARRB1) is involved in the desensitization of receptors by targeting them to clathrin-coated vesicles through a RhoA and actin-dependent mechanism (3). WASF2 is an important down-stream effector of receptor-mediated signaling that triggers actin polymerization. WASF family members also play important roles late in clathrin-coated pit formation by coupling to the ARP2/3 actin-regulating complex and may act to move the vesicle through the cell (35). This suggests a potential role of these genes in regulating RSV endocytosis after the binding of RSV receptors.

Consistent with a key role for endocytosis in RSV entry, specific siRNAs targeting genes known to be important in endocytosis itself were indicated. Most notable were those required for the assembly of clathrin-coated pits, including those encoding AP-2 subunits and clathrin light chain B. The alpha and beta subunits of AP-2 are important for clathrin-coated pit formation and are involved in clustering receptors to pit invaginations on the cell membrane. Clathrin light chains A and B are the main protein coating the cytoplasmic faces of clathrin-coated pits, and they control pit assembly. Together with clathrin heavy chains, the light chains form distinct structures, termed triskelions, upon which the clathrin coat is assembled (33). Multiple isoforms and variants of each of the clathrin light chain genes are expressed within the same cell at the same time. These variants are believed to have different roles in controlling the endocytosis kinetics and possibly the origins and destinations of cargoes (33).

The role of clathrin-mediated endocytosis was independently confirmed by chlorpromazine treatment of cells and by transfecting cells with a well-characterized dominant-negative mutant form of Eps15. Chlorpromazine treatment is reported to be a specific inhibitor of clathrin-mediated endocytosis (57), while Eps15 is a critical component of clathrin pit formation and interacts with both AP2-alpha and -beta (45). The dominant-negative form of Eps15 potently blocks the uptake of labeled transferrin by clathrin-mediated endocytosis but does not block other markers that are taken up by caveolae or macropinocytosis (4). Both the drug treatment and the expression of dominant-negative Eps15 were effective inhibitors of RSV infection. The major technical hurdle in using this and other dominant-negative genes is that the phenotypes are dosage dependent and require moderate- to high-level expression in cells. In the current work, FACS analysis was used to overcome this limitation while providing statistical power to the analysis. The results of the FACS analysis confirmed what was suggested by microscopy and showed a strong correlation between Eps15 Δ95–295 expression and a statistically significant decrease in the level of RSV infection. The drop in infection seen with chlorpromazine and the mutant Eps15 was similar to that seen for VSV, a virus characterized as using clathrin-mediated endocytosis (52). This observation, together with the siRNA data, strongly indicates a key role for clathrin function in RSV infection. However, this evidence alone does not indicate that endocytosis is also important, since clathrin is involved in other cellular functions, such as mitosis (43).

The confirmation that endocytosis was required for RSV infection was obtained by using siRNAs and dominant-negative mutants targeting the endocytic machinery itself. The primary siRNA screen indicated that targeting of the endocytosis-regulating proteins ITSN1 and -2, dynamin 3, and Rab5A each resulted in significant decreases in infection. Except for ITSN1, each was confirmed in the secondary screen using individual siRNAs instead of pools. Both the dynamin 3 suppression and Rab5 suppression were confirmed by Western blotting. Dynamins are involved in pinching off endocytic vesicles, including clathrin-coated pits and caveolae, from the cell membrane (13, 23). Intersectins (ITSN) bind dynamin and are involved in regulating clathrin-mediated endocytosis (40). Rab5 directly controls the formation of early endosomes. The dominant-negative mutant forms of Rab5 confirmed a need for early endosome formation for RSV infection. Interestingly, while the dominant-negative form suppressed infection by both RSV and the VSV control, the constitutively active form of Rab5 (Q79L) did not affect RSV infection greatly. The difference between these two mutant proteins of Rab5 is that the negative form blocks early endosome formation, whereas the active form enhances early endosome formation but disrupts down-stream maturation steps. These observations then suggest that, unlike VSV, RSV does not require steps immediately after early endosome formation or that another pathway not disrupted by the active mutant takes over. Caveolae are one such candidate. These endocytic vesicles intersect with the clathrin-dependent endosomes at the early endosome and play a role in JC virus infection (42). Indeed, siRNA targeting caveolin 2 had some effect on RSV infection but fell below the threshold of significance for the screen. However, the great preponderance of siRNAs targeting clathrin-related genes that had significant

effects on infection argues that if caveolae play a part in RSV infection, it must be at a step after the initial virus uptake into the cell. Additional studies with specific inhibitors of late endosomes, caveolae, and other early endosome markers will help to resolve this issue and determine the exact point of RSV exit from the endosomal pathway.

In this work, siRNAs that reduced infection were focused on and studied. Interestingly, treatment with some siRNAs elevated infection levels by as much as two- to threefold and included siRNAs targeting Stau, Bin1, AP1M2, and Rab7B genes. Stau is involved in RNA association with the cytoskeleton and could be important for the subcellular localization of the viral genome. Bin1 (amphiphysin 2) isoforms are involved in numerous processes, including endocytosis and cell cycle regulation (58), and AP1M2 is implicated in the regulation of clathrin-mediated endocytosis and for the basolateral sorting of receptors (17). Rab7 controls the maturation of late endosomes from early endosomes. Such genes, which raise the level of infection when suppressed, could be part of a host innate immune response against the virus, and could include PKR, which is an important mediator of the interferon response against RNA viruses (2), or APOBEC, which degrades retroviral nucleic acids upon entry into the cell cytoplasm (34). Suppressing the expression of each of these genes would be predicted to result in increased infection. However, the genes in the present screen are unlikely to be directly involved in known innate immunity pathways. Instead, it is more likely that at least Bin1 and AP1M2 are involved in regulating endocytic pathways that misdirect virus into parts of the cell that are not conducive for replication. Since Rab7 is key for late endosome formation, it is likely that reaching this compartment is deleterious to RSV. Consistent with this was the finding that the constitutively active Rab5 Q79L mutant, which blocks the maturation of early into late endosomes, did not inhibit RSV infection.

Among the siRNAs that targeted one of several isoforms or gene variants, typically one variant appeared more important for virus infection than others. Of the three Rab5 isoforms, three dynamins, three WASF variants, and two clathrin light chains targeted, only the Rab5A, dynamin 3, WASF2, and clathrin light chain B siRNA pools reduced infection below the cutoff threshold for the primary screen. The different activities of the Rab5, dynamin, and clathrin light chain variant-specific siRNAs were not due to lack of endogenous protein expression in the HeLa cells or lack of siRNA efficacy, since Western blots for at least Rab5A and 5B, as well as dynamin 2 and 3 and clathrin light chain A and B, were expressed and reduced to similar extents after siRNA treatment. Instead, the distinction may be that RSV prefers a pathway controlled by clathrin light chain B, dynamin 3, and Rab5A for optimal infection. Other similar pathways may operate in parallel, but subtle differences in the destination or the path taken by each may preclude virus from targeting sites needed for replication. Indeed, clathrin light chain A and B have been shown to have different kinetics of vesicle association and may control trafficking to different sites within the cell (1). This level of selectivity of a ligand for a specific gene isoform is not typical. In previous work, studying the endocytic trafficking requirements of the EGF receptor, only after suppression of the expression of all three isoforms of Rab5 was EGFR trafficking interrupted (25). It has been suggested by others that well-characterized viruses such as VSV and simian virus 40 may serve as superior probes for dissecting endocytic mechanisms (39). The current work and that of others indicate that viruses have very specific trafficking requirements. Virus-encoded reporter assays also have the advantage of signal amplification. Taking advantage of these strengths, we demonstrate that it is also possible to use an siRNA approach to define the entry mechanism of an uncharacterized virus such as RSV.

The current work highlights the power of using siRNAs to identify new genes and pathways important for pathogen infection. We chose to focus on a subset of genes important in endocytosis and actin rearrangement. While the screen did not exhaustively target all such genes, it had the advantage of yielding information for a workable set of genes that could be confirmed through independent tests. This approach and the methods of validation used in these studies were recently recommended by experts in the RNA interference (RNAi) field to limit the reporting of false positives from RNAi screens (16). The activity of siRNA pools was confirmed by testing individual siRNAs targeting the same gene, limiting potential false positives due to off-target effects. The next level of validation demonstrated that protein expression was specifically reduced after siRNA treatment. This portion of the work was limited by the availability of antibodies able to detect endogenous protein in cells. Independent tests using dominant-negative and constitutively active forms of proteins in the endocytic pathway then confirmed endocytosis as important for RSV. Larger (whole genome) siRNA screens will yield many potential genes involved in virus infection but will likely be hindered by off-target effects and means to independently validate hits. However, progress is being made toward increasing siRNA specificity, and an expanded repertoire of dominant-negative genes and specific drugs will make such screens increasingly effective for identifying potential targets of disease intervention.

ACKNOWLEDGMENTS

This work was supported in part by grants from National Institute of Allergy and Infectious Diseases to R.D. through the Western Regional Center of Excellence for Biodefense and Emerging Infectious Disease Research and NIH grants number U54 AI057156 and number 1R01AI063513-01A2.

We thank the UTMB Optical Imaging Center, and its manager Eugene Knutson for assistance in performing confocal microscopy. The UTMB cell sorting facility and staff helped in obtaining FACS data.

REFERENCES

1. **Acton, S. L., D. H. Wong, P. Parham, F. M. Brodsky, and A. P. Jackson.** 1993. Alteration of clathrin light chain expression by transfection and gene disruption. Mol. Biol. Cell **4:**647–660.
2. **Balachandran, S., P. C. Roberts, L. E. Brown, H. Truong, A. K. Pattnaik, D. R. Archer, and G. N. Barber.** 2000. Essential role for the dsRNA-dependent protein kinase PKR in innate immunity to viral infection. Immunity **13:**129–141.
3. **Barnes, W. G., E. Reiter, J. D. Violin, X. R. Ren, G. Milligan, and R. J. Lefkowitz.** 2005. β-Arrestin 1 and $G_{\alpha q/11}$ coordinately activate RhoA and stress fiber formation following receptor stimulation. J. Biol. Chem. **280:** 8041–8050.
4. **Benmerah, A., M. Bayrou, N. Cerf-Bensussan, and A. Dautry-Varsat.** 1999. Inhibition of clathrin-coated pit assembly by an Eps15 mutant. J. Cell Sci. **112:**1303–1311.
5. **Benmerah, A., C. Lamaze, B. Begue, S. L. Schmid, A. Dautry-Varsat, and N. Cerf-Bensussan.** 1998. AP-2/Eps15 interaction is required for receptor-mediated endocytosis. J. Cell Biol. **140:**1055–1062.
6. **Benmerah, A., V. Poupon, N. Cerf-Bensussan, and A. Dautry-Varsat.** 2000.

Mapping of Eps15 domains involved in its targeting to clathrin-coated pits. J. Biol. Chem. **275:**3288–3295.
7. **Blanchard, E., S. Belouzard, L. Goueslain, T. Wakita, J. Dubuisson, C. Wychowski, and Y. Rouille.** 2006. Hepatitis C virus entry depends on clathrin-mediated endocytosis. J. Virol. **80:**6964–6972.
8. **Bressanelli, S., K. Stiasny, S. L. Allison, E. A. Stura, S. Duquerroy, J. Lescar, F. X. Heinz, and F. A. Rey.** 2004. Structure of a flavivirus envelope glycoprotein in its low-pH-induced membrane fusion conformation. EMBO J. **23:**728–738.
9. **Bullough, P. A., F. M. Hughson, J. J. Skehel, and D. C. Wiley.** 1994. Structure of influenza haemagglutinin at the pH of membrane fusion. Nature **371:**37–43.
10. **Chandran, K., N. J. Sullivan, U. Felbor, S. P. Whelan, and J. M. Cunningham.** 2005. Endosomal proteolysis of the Ebola virus glycoprotein is necessary for infection. Science **308:**1643–1645.
11. **Cianci, C., N. Meanwell, and M. Krystal.** 2005. Antiviral activity and molecular mechanism of an orally active respiratory syncytial virus fusion inhibitor. J. Antimicrob. Chemother. **55:**289–292.
12. **Daecke, J., O. T. Fackler, M. T. Dittmar, and H. G. Krausslich.** 2005. Involvement of clathrin-mediated endocytosis in human immunodeficiency virus type 1 entry. J. Virol. **79:**1581–1594.
13. **Damke, H., T. Baba, D. E. Warnock, and S. L. Schmid.** 1994. Induction of mutant dynamin specifically blocks endocytic coated vesicle formation. J. Cell Biol. **127:**915–934.
14. **Delos, S. E., J. A. Godby, and J. M. White.** 2005. Receptor-induced conformational changes in the SU subunit of the avian sarcoma/leukosis virus A envelope protein: implications for fusion activation. J. Virol. **79:**3488–3499.
15. **Dharmawardhane, S., A. Schurmann, M. A. Sells, J. Chernoff, S. L. Schmid, and G. M. Bokoch.** 2000. Regulation of macropinocytosis by p21-activated kinase-1. Mol. Biol. Cell **11:**3341–3352.
16. **Echeverri, C. J., P. A. Beachy, B. Baum, M. Boutros, F. Buchholz, S. K. Chanda, J. Downward, J. Ellenberg, A. G. Fraser, N. Hacohen, W. C. Hahn, A. L. Jackson, A. Kiger, P. S. Linsley, L. Lum, Y. Ma, B. Mathey-Prevot, D. E. Root, D. M. Sabatini, J. Taipale, N. Perrimon, and R. Bernards.** 2006. Minimizing the risk of reporting false positives in large-scale RNAi screens. Nat. Methods **3:**777–779.
17. **Folsch, H., H. Ohno, J. S. Bonifacino, and I. Mellman.** 1999. A novel clathrin adaptor complex mediates basolateral targeting in polarized epithelial cells. Cell **99:**189–198.
18. **Gallina, A., T. M. Hanley, R. Mandel, M. Trahey, C. C. Broder, G. A. Viglianti, and H. J. Ryser.** 2002. Inhibitors of protein-disulfide isomerase prevent cleavage of disulfide bonds in receptor-bound glycoprotein 120 and prevent HIV-1 entry. J. Biol. Chem. **277:**50579–50588.
19. **Gibbons, D. L., B. Reilly, A. Ahn, M. C. Vaney, A. Vigouroux, F. A. Rey, and M. Kielian.** 2004. Purification and crystallization reveal two types of interactions of the fusion protein homotrimer of Semliki Forest virus. J. Virol. **78:**3514–3523.
20. **Goodman, O. B., Jr., J. G. Krupnick, F. Santini, V. V. Gurevich, R. B. Penn, A. W. Gagnon, J. H. Keen, and J. L. Benovic.** 1996. Beta-arrestin acts as a clathrin adaptor in endocytosis of the beta2-adrenergic receptor. Nature **383:**447–450.
21. **Gower, T. L., M. K. Pastey, M. E. Peeples, P. L. Collins, L. H. McCurdy, T. K. Hart, A. Guth, T. R. Johnson, and B. S. Graham.** 2005. RhoA signaling is required for respiratory syncytial virus-induced syncytium formation and filamentous virion morphology. J. Virol. **79:**5326–5336.
22. **Hallak, L. K., D. Spillmann, P. L. Collins, and M. E. Peeples.** 2000. Glycosaminoglycan sulfation requirements for respiratory syncytial virus infection. J. Virol. **74:**10508–10513.
23. **Henley, J. R., E. W. Krueger, B. J. Oswald, and M. A. McNiven.** 1998. Dynamin-mediated internalization of caveolae. J. Cell Biol. **141:**85–99.
24. **Hernandez, L. D., L. R. Hoffman, T. G. Wolfsberg, and J. M. White.** 1996. Virus-cell and cell-cell fusion. Annu. Rev. Cell Dev. Biol. **12:**627–661.
25. **Huang, F., A. Khvorova, W. Marshall, and A. Sorkin.** 2004. Analysis of clathrin-mediated endocytosis of epidermal growth factor receptor by RNA interference. J. Biol. Chem. **279:**16657–16661.
26. **Hussain, N. K., S. Jenna, M. Glogauer, C. C. Quinn, S. Wasiak, M. Guipponi, S. E. Antonarakis, B. K. Kay, T. P. Stossel, N. Lamarche-Vane, and P. S. McPherson.** 2001. Endocytic protein intersectin-l regulates actin assembly via Cdc42 and N-WASP. Nat. Cell Biol. **3:**927–932.
27. **Jackson, A. L., S. R. Bartz, J. Schelter, S. V. Kobayashi, J. Burchard, M. Mao, B. Li, G. Cavet, and P. S. Linsley.** 2003. Expression profiling reveals off-target gene regulation by RNAi. Nat. Biotechnol. **21:**635–637.
28. **Kahn, J. S., M. J. Schnell, L. Buonocore, and J. K. Rose.** 1999. Recombinant vesicular stomatitis virus expressing respiratory syncytial virus (RSV) glycoproteins: RSV fusion protein can mediate infection and cell fusion. Virology **254:**81–91.
29. **Karron, R. A., D. A. Buonagurio, A. F. Georgiu, S. S. Whitehead, J. E. Adamus, M. L. Clements-Mann, D. O. Harris, V. B. Randolph, S. A. Udem, B. R. Murphy, and M. S. Sidhu.** 1997. Respiratory syncytial virus (RSV) SH and G proteins are not essential for viral replication in vitro: clinical evaluation and molecular characterization of a cold-passaged, attenuated RSV subgroup B mutant. Proc. Natl. Acad. Sci. USA **94:**13961–13966.
30. **Kolokoltsov, A. A., E. H. Fleming, and R. A. Davey.** 2006. Venezuelan equine encephalitis virus entry mechanism requires late endosome formation and resists cell membrane cholesterol depletion. Virology **347:**333–342.
31. **Lehmann, M. J., N. M. Sherer, C. B. Marks, M. Pypaert, and W. Mothes.** 2005. Actin- and myosin-driven movement of viruses along filopodia precedes their entry into cells. J. Cell Biol. **170:**317–325.
32. **Levine, S., R. Klaiber-Franco, and P. R. Paradiso.** 1987. Demonstration that glycoprotein G is the attachment protein of respiratory syncytial virus. J. Gen. Virol. **68:**2521–2524.
33. **Loerke, D., M. Wienisch, O. Kochubey, and J. Klingauf.** 2005. Differential control of clathrin subunit dynamics measured with EW-FRAP microscopy. Traffic **6:**918–929.
34. **Mangeat, B., P. Turelli, G. Caron, M. Friedli, L. Perrin, and D. Trono.** 2003. Broad antiretroviral defence by human APOBEC3G through lethal editing of nascent reverse transcripts. Nature **424:**99–103.
35. **Merrifield, C. J., B. Qualmann, M. M. Kessels, and W. Almers.** 2004. Neural Wiskott Aldrich syndrome protein (N-WASP) and the Arp2/3 complex are recruited to sites of clathrin-mediated endocytosis in cultured fibroblasts. Eur. J. Cell Biol. **83:**13–18.
36. **Nabi, I. R., and P. U. Le.** 2003. Caveolae/raft-dependent endocytosis. J. Cell Biol. **161:**673–677.
37. **Naslavsky, N., R. Weigert, and J. G. Donaldson.** 2004. Characterization of a nonclathrin endocytic pathway: membrane cargo and lipid requirements. Mol. Biol. Cell **15:**3542–3552.
38. **Pelkmans, L., T. Burli, M. Zerial, and A. Helenius.** 2004. Caveolin-stabilized membrane domains as multifunctional transport and sorting devices in endocytic membrane traffic. Cell **118:**767–780.
39. **Pelkmans, L., and A. Helenius.** 2003. Insider information: what viruses tell us about endocytosis. Curr. Opin. Cell Biol. **15:**414–422.
40. **Pucharcos, C., X. Estivill, and S. de la Luna.** 2000. Intersectin 2, a new multimodular protein involved in clathrin-mediated endocytosis. FEBS Lett. **478:**43–51.
41. **Pullan, C. R., and E. N. Hey.** 1982. Wheezing, asthma, and pulmonary dysfunction 10 years after infection with respiratory syncytial virus in infancy. Br. Med. J. Clin. Res. **284:**1665–1669.
42. **Querbes, W., B. A. O'Hara, G. Williams, and W. J. Atwood.** 2006. Invasion of host cells by JC virus identifies a novel role for caveolae in endosomal sorting of noncaveolar ligands. J. Virol. **80:**9402–9413.
43. **Royle, S. J., N. A. Bright, and L. Lagnado.** 2005. Clathrin is required for the function of the mitotic spindle. Nature **434:**1152–1157.
44. **Scaplehorn, N., A. Holmstrom, V. Moreau, F. Frischknecht, I. Reckmann, and M. Way.** 2002. Grb2 and Nck act cooperatively to promote actin-based motility of vaccinia virus. Curr. Biol. **12:**740–745.
45. **Schmid, E. M., M. G. Ford, A. Burtey, G. J. Praefcke, S. Y. Peak-Chew, I. G. Mills, A. Benmerah, and H. T. McMahon.** 2006. Role of the AP2 beta-appendage hub in recruiting partners for clathrin-coated vesicle assembly. PLoS Biol. **4:**e262.
46. **Schweizer, A., J. A. Fransen, T. Bachi, L. Ginsel, and H. P. Hauri.** 1988. Identification, by a monoclonal antibody, of a 53-kD protein associated with a tubulo-vesicular compartment at the cis-side of the Golgi apparatus. J. Cell Biol. **107:**1643–1653.
47. **Smith, J. G., W. Mothes, S. C. Blacklow, and J. M. Cunningham.** 2004. The mature avian leukosis virus subgroup A envelope glycoprotein is metastable, and refolding induced by the synergistic effects of receptor binding and low pH is coupled to infection. J. Virol. **78:**1403–1410.
48. **Srinivasakumar, N., P. L. Ogra, and T. D. Flanagan.** 1991. Characteristics of fusion of respiratory syncytial virus with HEp-2 cells as measured by R18 fluorescence dequenching assay. J. Virol. **65:**4063–4069.
49. **Stein, B. S., S. D. Gowda, J. D. Lifson, R. C. Penhallow, K. G. Bensch, and E. G. Engleman.** 1987. pH-independent HIV entry into CD4-positive T cells via virus envelope fusion to the plasma membrane. Cell **49:**659–668.
50. **Stenmark, H., R. G. Parton, O. Steele-Mortimer, A. Lutcke, J. Gruenberg, and M. Zerial.** 1994. Inhibition of rab5 GTPase activity stimulates membrane fusion in endocytosis. EMBO J. **13:**1287–1296.
51. **Suetsugu, S., D. Yamazaki, S. Kurisu, and T. Takenawa.** 2003. Differential roles of WAVE1 and WAVE2 in dorsal and peripheral ruffle formation for fibroblast cell migration. Dev. Cell **5:**595–609.
52. **Sun, X., V. K. Yau, B. J. Briggs, and G. R. Whittaker.** 2005. Role of clathrin-mediated endocytosis during vesicular stomatitis virus entry into host cells. Virology **338:**53–60.
53. **Techaarpornkul, S., N. Barretto, and M. E. Peeples.** 2001. Functional analysis of recombinant respiratory syncytial virus deletion mutants lacking the small hydrophobic and/or attachment glycoprotein gene. J. Virol. **75:**6825–6834.
54. **Teng, M. N., and P. L. Collins.** 1998. Identification of the respiratory syncytial virus proteins required for formation and passage of helper-dependent infectious particles. J. Virol. **72:**5707–5716.
55. **Walsh, E. E., and J. Hruska.** 1983. Monoclonal antibodies to respiratory syncytial virus proteins: identification of the fusion protein. J. Virol. **47:**171–177.
56. **Wang, C., K. Takeuchi, L. H. Pinto, and R. A. Lamb.** 1993. Ion channel

activity of influenza A virus M2 protein: characterization of the amantadine block. J. Virol. **67:**5585–5594.

57. **Wang, L. H., K. G. Rothberg, and R. G. Anderson.** 1993. Mis-assembly of clathrin lattices on endosomes reveals a regulatory switch for coated pit formation. J. Cell Biol. **123:**1107–1117.
58. **Wechsler-Reya, R. J., K. J. Elliott, and G. C. Prendergast.** 1998. A role for the putative tumor suppressor Bin1 in muscle cell differentiation. Mol. Cell. Biol. **18:** 566–575.
59. **Werling, D., J. C. Hope, P. Chaplin, R. A. Collins, G. Taylor, and C. J. Howard.** 1999. Involvement of caveolae in the uptake of respiratory syncytial virus antigen by dendritic cells. J. Leukoc. Biol. **66:**50–58.
60. **Wilson, I. A., J. J. Skehel, and D. C. Wiley.** 1981. Structure of the haemagglutinin membrane glycoprotein of influenza virus at 3 Å resolution. Nature **289:**366–373.
61. **Zhang, L., M. E. Peeples, R. C. Boucher, P. L. Collins, and R. J. Pickles.** 2002. Respiratory syncytial virus infection of human airway epithelial cells is polarized, specific to ciliated cells, and without obvious cytopathology. J. Virol. **76:**5654–5666.